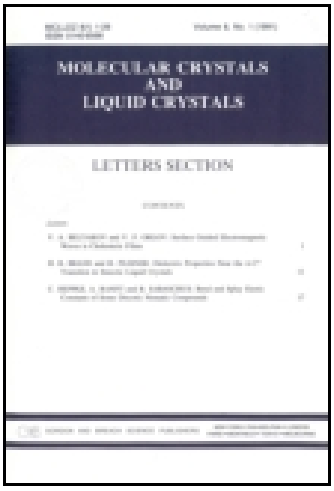

Molecular Crystals and Liquid Crystals
Publication details, including instructions for authors and subscription information:
http://www.tandfonline.com/loi/gmcl20

Deprotonation/Protonation Induced Spectral Switching of 1,8-Naphthalimide Dye

Xiaochuan Li[a], Yatian Zhang[a], Nan Zhao[a] & Young-A Son[b]
[a] School of Chemistry and Chemical Engineering, Henan Normal University, China
[b] BK21, Department of Advanced Organic Materials Engineering, Chungnam National University, South Korea
Published online: 17 Nov 2014.

To cite this article: Xiaochuan Li, Yatian Zhang, Nan Zhao & Young-A Son (2014) Deprotonation/Protonation Induced Spectral Switching of 1,8-Naphthalimide Dye, Molecular Crystals and Liquid Crystals, 600:1, 163-169, DOI: 10.1080/15421406.2014.937285

To link to this article: http://dx.doi.org/10.1080/15421406.2014.937285

Mol. Cryst. Liq. Cryst., Vol. 600: pp. 163–169, 2014

ISSN: 1542-1406 print/1563-5287 online
DOI: 10.1080/15421406.2014.937285

Taylor & Francis
Taylor & Francis Group

Deprotonation/Protonation Induced Spectral Switching of 1,8-Naphthalimide Dye

XIAOCHUAN LI,[1,*] YATIAN ZHANG,[1] NAN ZHAO,[1] AND YOUNG-A SON[2,*]

[1]School of Chemistry and Chemical Engineering, Henan Normal University, China
[2]BK21, Department of Advanced Organic Materials Engineering, Chungnam National University, South Korea

In this contribution, a new sensitive colorimetric chemosensors based naphthalimide was synthesized and characterized by NMR and mass spectroscopic techniques. Upon the addition of OH-, the solution of dye change its color from yellowish to deep blue, which can be easily observed by naked eye. The sensors show good selective against other common anions, including strong Lewis base F^-. The effects of deprotonation/protonation imposed on absorption spectrum were investigated. Further quantum chemical calculation uncovered the underlying signal mechanism. The lowered energy gap between HOMO/LUMO in NB-H leads to the longest maximum absorption (665 nm).

Keywords Chemosensors; naphthalimide; deprotonation/protonation; quantum chemical calculation

Introduction

1,8-Naphthalimide is a typical chromophores and widely employed as basic framework in constructing of various chemosensors, emitters, device, and light absorbers [1–6]. Recently, the research is focused on the construction of chemosensors for biological application [1, 2, 7–9]. 1,8-Naphthalimide can be conveniently synthesized from the corresponding 1,8-naphthalic anhydrides by ammoniation. This facilitates the production and design of a large number family of derivatives. Additionally, the framework of 1,8-naphthalimide is easy to be modified chemically, typically, substitution at the 3- or 4-position by amino or nitro groups. This not only allows the introduction of various functional groups, which can be used for targeting biomolecules, but also can have a major effect on the electronic properties with a consequent influence on the optical and photophysical properties [3]. Most of the 1,8-naphthalimide derivatives are strongly fluorescent with a marked Stokes

*Address correspondence to Prof. Xiaochuan Li, School of Chemistry and Chemical Engineering, Henan Normal University, East Jianshe Rd. 46, Xinxiang, Henan, 453007, China. Tel./Fax: 86-373-3323016. E-mail: lixiaochuan@henannu.edu.cn

*Address correspondence to Prof. Young-A Son, Department of Advanced Organic Materials Engineering, Chungnam National University, 220 Gung-dong, Daejeon, 305-764, South Korea. Tel.: 82-42-8216620; Fax: 82-42-821-8870. E-mail: yason@cnu.ac.kr

Color versions of one or more of the figures in the article can be found online at www.tandfonline.com/gmcl.

shift. The emission is of in the green part and can be modulated further towards to red or blue by altering the nature of the ring substituent or that of the imide. This opens up the door in various applications. Another important feature of 1,8-naphthalimides is that its derivatives are easy to synthesis in high purity on a large scale.

The molecular design, in this contribution, a receptor unit is introduced, which facilitated the internal charge transfer from the electron-rich naphthalene to the electron deficient imide when binding with analyte (cation, anion, or H^+) [10, 11]. Platform of the photoinduced electron transfer (**PET**) or photoinduced charge transfer (**PCT**) could be established based on the alternation of intramolecular electron density. In lines of this model construction, a Schiff base unit –NHNPh was introduced. Effective binding occurring to the NH unit is going to influence the electron properties of this dye. The remarkable photophysical properties induced by the electronic interaction is deserve to be investigated.

Experimental

General Procedures and Materials

All solvents used in reaction were carefully dried according to the standard procedure and stored over 4Å molecular sieve. All the reagent-grade chemicals were purchased from Aldrich and used without further purification. Melting points were determined on a Mel-Temp® IA9200 digital melting point apparatus in a glass capillary and were uncorrected. All synthesized compounds were routinely checked by TLC and ^{1}H NMR. TLC was performed on aluminum-backed silica gel plates (Merck DC. Alufolien Kieselgel 60 F254).

^{1}H and ^{13}C NMR Spectroscopy

^{1}H and ^{13}C nuclear magnetic resonance (NMR) spectra were recorded on a Brucker AM-400 spectrometer operating at frequencies of 400 MHz for proton 100 MHz for carbon in DMSO-d_6. Proton chemical shifts (δ) are relative to tetramethylsilane (TMS, $\delta = 0$) as internal standard and expressed in parts per million. Spin multiplicities are given as *s* (singlet), *d* (doublet), *t* (triplet), and *m* (multiplet) as well as *b* (broad). Coupling constants (*J*) are given in Hertz.

Mass and High Resolution Mass Spectra (HRMS)

Mass spectra measured on a LC-MS (Waters UPLC-TQD) mass spectrometer. High resolution mass spectra (HRMS) were measured on Brucker microOTOF II Focus instrument.

UV-Vis Spectra

Absorption spectra were measured with PERSEE TU-1900 and Agilent 8453 spectrophotometer. Emission spectra were measured with Shimadzu RF-5301PC fluorescence spectrophotometer. Solvents used in photochemical measurement were spectroscopic grade and were purified by distillation. The stock solution of compounds (2×10^{-3} M) was prepared in THF, and a fixed amount of these concentrated solutions were added to each experimental solution. All the experiments were done repeatedly, and reproducible results were obtained. Prior to the spectroscopic measurements, solutions were deoxygenated by bubbling nitrogen through them.

Theoretical Calculations

For the theoretical study of excited state photo-physics of the compound, the *DMol*[3] program packaged in *Material Studio* was used. The ground state geometries and the frontier molecular orbital of the compound were calculated using the density function theory (DFT) with the B3LYP hybrid functional and the double numerical plus *d*-functions (DND) atomic orbital basis set.

Synthesis

Synthetic routes of the target compound, 2-butyl-6-(2-(4-nitrobenzylidene)hydrazinyl)-benzo[*de*] isoquinoline-1,3-dione (**NB**), are outlined in Scheme 1. 4-bromo-1,8-naphthalic anhydride (**1**) is commercially available and purchased from Aldrich and used without further purification. Compound **2** (*N*-butane-4-bromo-1,8-naphthalimide) was synthesized following the procedure mentioned in the synthesis scheme described earlier [12]. The active bromine atom of compound **2** was substituted by nitrogen atom of hydrazine hydrate and gave **3** [13]. The NMR spectra were identical to the literature reported. **3** condensed with 4-nitrobenzaldehyde yielding **NB**.

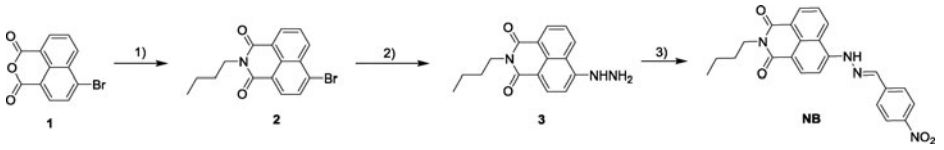

Scheme 1. Synthesis of 2-butyl-6-(2-(4-nitrobenzylidene)hydrazinyl)-benzo[de]isoquinoline-1,3-dione (**NB**). 1) *n*-$BuNH_2$, ethanol, reflux 4h; 2) NH_2NH_2, 2-methoxyethanol, reflux; 3) 4-nitrobenzaldehyde, methanol, r.t

2-Butyl-6-hydrazinyl-1,8-naphthalimide (73 mg, 0.26 mmol) and 4-nitrobenzaldehyde (39 mg, 0.26 mmol) dissolved in methanol (10 mL). The mixture was stirred at room temperature. Gradually, a large amount of yellow solid was formed. The precipitant was separated out. Pure compound was obtained by recrystallization from ethanol (101 mg, yield, 94 %).

^{1}H NMR (400 MHz, $CDCl_3$): δ 11.71 (*s*, 1H, -*NH*-), 8.74 (*d*, $J = 8.0$ Hz, 1H), 8.44 (*d*, $J = 8.0$ Hz, 2H), 8.36 (*d*, $J = 8.0$ Hz, 1H), 8.25 (*d*, $J = 8.0$ Hz, 2H), 7.98 (*d*, $J = 8.0$ Hz, 2H), 7.78 (*q*, $J = 8.0$ Hz, 2H), 4.00 (*t*, $J = 8.0$ Hz, 2H, -NCH_2-), 1.60 (*t*, $J = 8.0$ Hz, 2H, $CH_3CH_2CH_2$-), 1.35 (q, $J = 8.0$ Hz, 2H, CH_3CH_2-), 0.93 (*t*, $J = 8.0$ Hz, 3H, $-CH_3$); ^{13}CNMR (100 MHz, $CDCl_3$): δ 164.1, 163.5, 147.8, 141.6, 139.0, 133.7, 131.4, 130.0, 129.5, 128.7, 127.9, 125.9, 124.6, 122.6, 119.4, 112.7, 108.2, 30.2, 20.3, 18.9, 14.2. EI/MS m/z 416[M]$^+$. HRMS calcd for $C_{23}H_{20}N_4O_4$ 416.1485, found 416.1487.

Result and Discussion

NB showed the intense absorption peak located at 470 nm, which corresponds to the intramolecular charge transfer process of nitrogen atom substituted naphthalimide moiety. The effects of deprotonation and protonation on the colorimetric, chemosensing properties of a 2.0×10^{-5} M solution of **NB** in DMF were investigated. The titration spectra of OH^- were shown in Fig. 1. Upon the addition of OH^-, the longest absorption maximum at 470nm decreased and a new peak at 665 nm appeared with the isosbestic point at 382 and 515 nm, which indicates only two species co-exist in the equilibrium. There is a

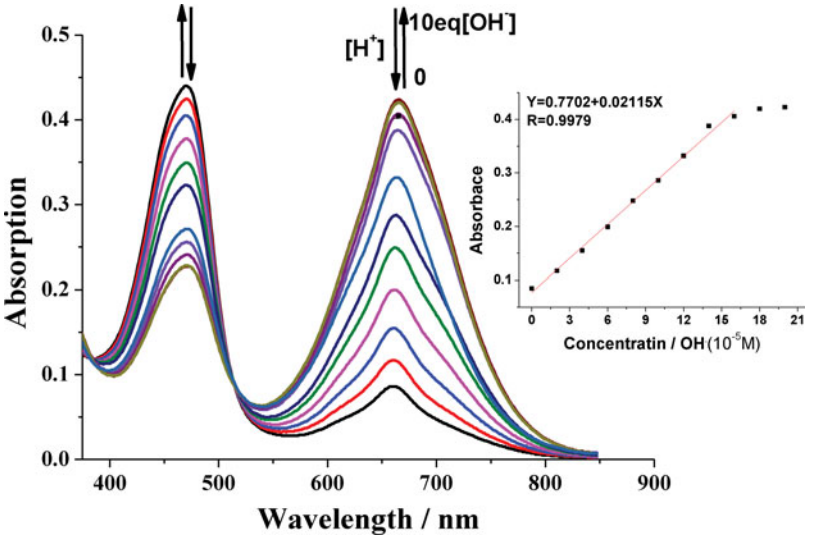

Figure 1. Absorption change of **NB** in DMF solution (2.0×10^{-5} M) imparted by deprotonation and protonation. Insert: dependence of absorption in intensity at 665 nm with respect to concentrations of OH^- ion.

slightly red-shift (5 nm) in the longest maximum absorption peak accompanied with the increasing of intensity. At the same time, the color of the solution changed from yellowish to blue gradually. A satisfactory linear relationship between absorption intensity and OH^- concentration was observed with the correlation coefficient as high as 0.9979 with the OH^- concentration varied from 0 to 8 equivalent, supporting effective interaction between OH^- and proton of –NH–. Upon addition of H^+, the blue color faded, and recovering the yellowish color. This blue/yellowish color transformation was reversible by the addition of OH^-/H^+. However, the typical green emission was not observable before and after the addition of base. The quantum yield of **NB** in solution state was estimated to be lower than 1%. There is no fluorescence enhancement observed by the addition of OH^-/H^+. The observed base–induced single changes in absorption behavior of **NB** can be attributed to the deprotonation of the dye **NB**. It has been demonstrated that aryl hydrazones derivatives of *N*-alkyl-1,8-naphthalimide were fluorescent with electron donor group attached (alkoxy). On the contrary, it was not fluorescence with electron-withdrawing group attached (-NO_2). Detailed analysis of the electronic effects of substituents on the physical properties was evaluated [14].

The effect of deprotonation from nitrogen atom by other anions was also tested. Apart from OH^-, no observable absorption change was found induced by other anions, such as Cl^-, Br^-, I^-, SO_4^{2-}, NO_3^-, $H_3PO_4^-$, CO_3^{2-}, ClO_4^-, and CO_3^{2-}. Even if the strong Lewis F^- was incubated, the proton of nitrogen atom can not be captured. Figure 2 shows the binding property toward different anions. The absorption enhancement at 665 nm induced by the same amount (10 μM) of OH^- was estimated to be 7-fold (F^-). Because of the small difference in size between fluorine and hydrogen, the molecular topology is not altered greatly, and hence little affection would be expected in the absorption spectra. The proposed combining mode was shown in Scheme 2. The occurrence of N–H deprotonation increases the electron density on the nitrogen atom, resulting in the enhancement of charger transfer process and red-shift of the absorption band. It should be noted that the deprotonation effect by OH^- is different from the hydrazones derivatives of *N*-alkyl-1,8-naphthalimide [10, 15].

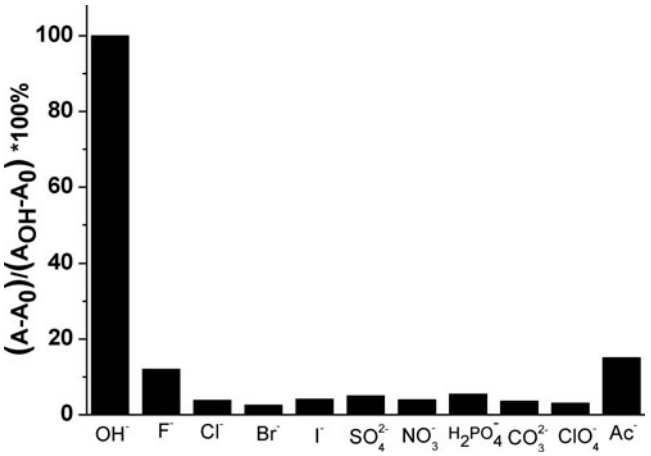

Figure 2. Comparison of percent increase of absorption of **NB** in DMF solution at 665 nm in the presence of 1equiv different anions.

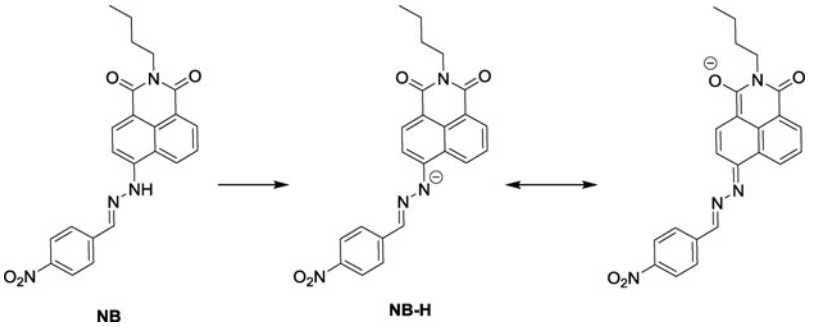

Scheme 2. Concept of deprotonation.

To better comprehend the geometrical, electronic, and optical properties of **NB**, we undertook a comprehensive computational investigation using Material Studio. To reduce the run times in the first instance, the ground-state energy-minimized structures were calculated using DFT and LDA/DN basis set [16, 17].

The size and signs of frontier molecules orbitals are illustrated in Fig. 3. According to the calculation, the transition HOMO→LUMO+1 and HOMO→LUMO+2 are possible with the oscillator strength (*f*) 0.295 and 0.234, respectively. The main absorption of **NB** calculated to be 478 nm (HOMO→LUMO+1), which is in good agreement with the experimentally observed absorption at 470 nm. After the proton of nitrogen atom was captured, the transition HOMO→LUMO is possible with the oscillator strength (*f*) 0.935. This transition corresponds to the calculated absorption 665 nm, which is also identical to the experimental value (665 nm). For **NB**, the electron density distributed over naphthalene unit in HOMO. The electron density increased in **NB−H** with the proton departed. Due to the withdraw effect of nitro, the electron density also shifted direct nitro in **NB−H**. With respect to the energy level of **NB** in HOMO (−5.21 eV), it was elevate to higher energy level (−1.54 eV). Similar distribution model was found in LUMO of **NB** and **NB−H**. However, the energy level for LUMO of **NB−H** was elevated higher. In contrast, the electron distribution in HOMO/LUMO is more even in **NB** than that of **NB−H**. Such

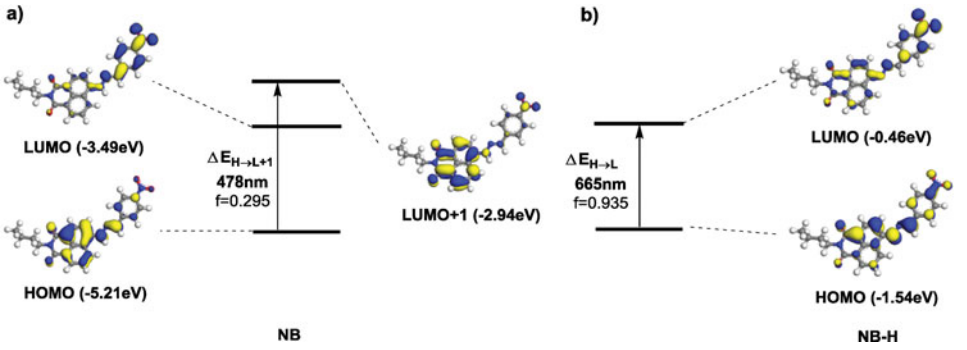

Figure 3. Electron density distributions and energies of the frontier orbitals of **NB** and **NB−H**.

location results the lower energy gap between HOMO/LUMO in **NB−H**. Therefore, the absorption shifted to longer wavelength (665 nm) once the proton departed from the nitrogen. The increased electron density located on nitrogen atom enhanced the charger transfer process from naphthalene unit to nitrobenzene unit.

Conclusions

In summary, a new 2-butyl-6-(2-(4-nitrobenzylidene)hydrazinyl)-benzo[*de*]isoquinoline-1,3-dione dye was synthesized and fully characterized. Its effect of deprotonation was investigated in detail. Upon the OH^- addition, the absorption peak at 470 nm decreased and a new peak around 665 nm appeared. At the same time, the solution changed from yellowish to deep blue gradually. Deprotonation of NH results a significant increase of electron density located at nitrogen atom. The calculated absorption for **NB** and **NB−H** are in agreement with the experimental values. Enhanced intramolecular charge transfer leads to the lower energy gap between HOMO/LUMO in **NB−H**.

Funding

This work was supported by the National Natural Science Foundation of China (grant no. 21072048 and 21272060). This research was supported by the Basic Science Research Program through the National Research Foundation of Korea (NRF) funded by the Ministry of Education, Science and Technology (grant no. 2013054767).

References

[1] Zhang, J. F., Kim, S., Han, J. H., Lee, S.-J., Pradhan T., Cao, Q. Y., Lee S. J., Kang, C., & Kim, J. S. (2011). *Org. Lett.*, *13*, 5294.
[2] Veale E. B., & Gunnlaugsson T. (2011). *J. Org. Chem.*, *75*, 5513.
[3] Coronado, J. L. G., Martın, E., Montero, L. A., Fierro, J. L. G., & Garcı'a de la Vega, J. M. (2007). *J. Phys. Chem. A*, *111*, 9724.
[4] Gan, J. A., Song, Q. L., Hou, X. Y., Chen, K., & Tian, H. (2004). *J. Photochem. Photobiolo. A Chemistry*, *162*, 399.
[5] Cho, D. W., Fujitsuka, M., Choi, K. H., Park, M. J., Yoon, U. C., & Majima, T. (2006). *J. Phys. Chem. B*, *110*, 4576.
[6] Pogozhev, D. V., Bezdek, M. J., Schauer, P. A., & Berlinguette, C. P. (2013). *Inorg. Chem.*, *52*, 3001.

[7] Kilpin, K. J., Clavel, C. M., Edafe, F., & Dyson, P. J. (2012). *Organometallics*, *31*, 7031.
[8] Lee, M. H., Kim, J. Y., Han, J. H., Bhuniya, S., Sessler, J. L., Kang, C., & Kim, J. S. (2012). *J. Am. Chem. Soc.*, *134*, 12668.
[9] Banerjee, S., Veale, E. B., Phelan, C. M., Murphy, S. A., Tocci, G. M., Gillespie, L. J., Frimannsson, D. O., Kelly, J. M., & Gunnlaugsson, T. (2013). *Chem. Soc. Rev.*, *42*, 1601.
[10] Li, X., Zhu, K., Jiang, W., Li, Y., Kim, H., & Son, Y. (2012). *Phys. Status. Solidi. C*, *9*, 2456.
[11] Yang, H., Song, H., Zhu, Y., & Yang, S. (2012). *Tetrahedron Lett.*, *53*, 2026.
[12] Wang, J., Xu, Z., Zhao, Y., Qiao, W., & Li, Z. (2007). *Dyes Pigments*, *74*, 103.
[13] Gan, J., Tian, H., Wang, Z. H., Chen, K. C., Hill, J., Lane, P. A., Rahn, M. D., Fox, A. M., & Bradley, D. D. C. (2002). *J. Organomet. Chem.*, *645*, 168.
[14] Ivanov, I. P., Dimitrova, M. B., Tasheva, D. N., Cheshmedzhieva, D. V., Lozanov, V. S., & Ilieva, S. V. (2013). *Tetrahedron*, *69*, 712.
[15] Yang, H., Song, H., Zhu, Y., & Yang, S. (2012). *Tetrahedron Lett.*, *53*, 2026.
[16] Delley, B. (1990). *J. Chem. Phys.*, *92*, 508.
[17] Delley, B. (2000). *J. Chem. Phys.*, *113*, 7756.